

# High-resolution synchrotron X-ray powder diffraction study of bis(2-methylimidazolyl)-zinc, $C_8H_{10}N_4Zn$ (ZIF-8)

W. Wong-Ng<sup>a)</sup>

Ceramics Division, NIST, Gaithersburg, Maryland 20899

J. A. Kaduk

Poly Crystallography Inc., Naperville, Illinois 60540

L. Espinal

Ceramics Division, NIST, Gaithersburg, Maryland 20899

M. R. Suchomel

Advanced Photon Source, Argonne National Laboratory, Argonne, Illinois 60439

A. J. Allen

Ceramics Division, NIST, Gaithersburg, Maryland 20899

H. Wu

NIST Center for Neutron Research (NCNR), Gaithersburg, Maryland 20899

(Received 17 November 2010; accepted 8 February 2011)

The family of zeolitic imidazolate framework (ZIF) compounds is efficient sorbent materials that can be used for catalytic, ion exchange, gas storage, and gas separation applications. A high-resolution reference X-ray powder diffraction pattern for one of the ZIF members, bis(2-methylimidazolyl)-zinc,  $C_8H_{10}N_4Zn$  (commonly known as ZIF-8), was determined using synchrotron diffraction data obtained at the Advanced Photon Source (APS) in Argonne, IL. The sample was confirmed to be cubic  $I-43m$ , with  $a = 17.01162(6)$  Å,  $V = 4932.08$  Å<sup>3</sup>, and  $Z = 12$ . The reference X-ray powder diffraction pattern has been submitted for inclusion in the Powder Diffraction File (PDF). © 2011 International Centre for Diffraction Data. [DOI: 10.1154/1.3625701]

Key words: zeolite, ZIF-8, synchrotron diffraction, reference XRD pattern, PDF

## I. INTRODUCTION

An increase of carbon dioxide in the atmosphere, which mainly comes from fossil fuel emissions from energy production processes, is considered a major contributor to global climate change, rising sea levels, and increased acidity of oceans. As coal-burning power plants will be an important part of energy production in the foreseeable future, reducing emissions from these plants is critical for global sustainability.

For carbon capture applications, there have been intensive efforts to develop new classes of zeolite-like materials based upon porous metal-organic framework (MOF) materials (Wang *et al.*, 2008a; Park *et al.* 2006; Britt *et al.*, 2008; Chapman *et al.*, 2009; Pérez-Pellitero *et al.*, 2010). The salient structural features of MOFs are large pores with small apertures that are essential in catalytic, ion-exchange, gas storage, and gas separation applications. Current MOF research is focused on incorporating different transition metal ions and organic units into the framework structure, with the goal of modifying the pore size and shape in these materials, and identifying new or improved catalytic and adsorption properties.

Zeolitic imidazolate framework (ZIF) materials are a new class of MOF materials that use imidazolate ligands to bind to tetrahedral  $M(II)$  ions ( $M = Co, Cu, Zn, Mg$ , etc.) (Park *et al.* 2006; Lewis *et al.*, 2009; Wu *et al.*, 2007). These are porous crystalline materials with a cage-like tetrahedral network. In the ZIF architecture,  $M^{2+}$  ions typically play the

role of silicon, and the imidazolate anions form bridges that mimic the role of oxygen in natural aluminosilicate zeolites. The resulting structure provides bond angles that are similar to those found for Si-O-Si in zeolites.

Bis(2-methylimidazolyl)-zinc,  $C_8H_{10}N_4Zn$  or  $(CH_3C_3H_2N_2)_2Zn$  (commonly known as the ZIF-8), is one of the 20 ZIF family members that were first reported by Park *et al.* (2006). ZIFs have been reported to readily adsorb  $H_2$  and  $CO_2$ . Their tunable pore size and high thermal stability are a result of the strong bonding between the imidazolate linker and the metal center. It was reported by Wu *et al.* (2007) that at high  $H_2$  loading, the ZIF-8 structure is capable of holding up to 28  $H_2$  molecules (4.2% mass fraction). This material also has high-capture efficiency for  $CO_2$  (Wang *et al.*, 2008a; Park *et al.*, 2006).

As X-ray powder diffraction is a nondestructive method for characterization, determination of standard reference diffraction patterns for sorbent materials plays a critical role for the research community that investigates efficient solid sorbent materials for the  $CO_2$  capture process. We report the high-resolution experimental powder diffraction pattern for the ZIF-8 material for inclusion in the Powder Diffraction File (PDF).

## II. EXPERIMENTAL<sup>1</sup>

The ZIF-8 sample was obtained from Sigma-Aldrich Chemical Corp. under the commercial name of Basolite

<sup>a)</sup>Author to whom correspondence should be addressed. Electronic mail: winnie.wong-ng@nist.gov

<sup>1</sup>The purpose of identifying the chemical and equipment in this article is to specify the experimental procedure. Such identification does not imply recommendation or endorsement by the National Institute of Standards and Technology.

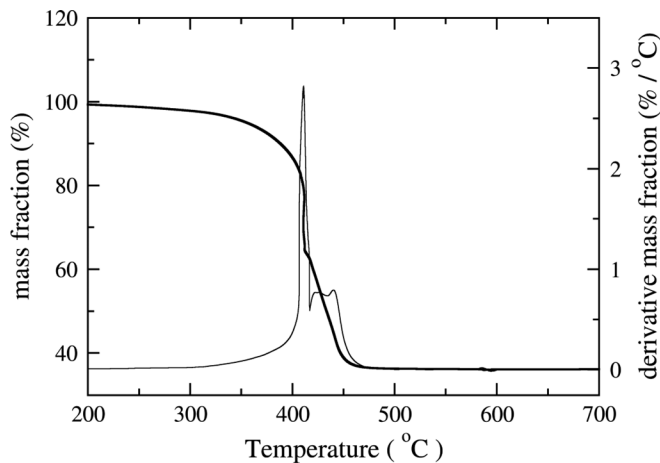


Figure 1. Thermogravimetric analysis of ZIF-8 up to 1000 °C.

Z1200 (Lot S45328-308). Sample loading into the capillaries used for data collection was performed inside a dry box with flowing Ar. Activation of ZIF-8 was performed under vacuum at 200 °C for 2 h. The thermal stability of the sample was studied using thermogravimetric analysis (TGA). Figure 1 shows the TGA results of ZIF-8 up to 1000 °C. The thermal stability of the sample was established up to about 350 °C. The X-ray pattern of the sample heat-treated at 500 °C indicates that this sample has decomposed mainly to ZnO.

Small-angle neutron scattering (SANS) measurements were made on a small amount of ZIF-8 powder encapsulated between two layers of a polyamide film (Glinka *et al.*, 1998). The SANS measurements indicate porous features of 100 Å and larger within the powder grains. Depending on the uncertain powder packing density, these pores comprise 3 to 4% of the sample volume and have an associated surface area of 8 to 12 m<sup>2</sup>/cm<sup>3</sup>. While not affecting the high-

resolution XRD structure analysis (and separate from the 11.6-Å porosity detected by XRD), this intermediate pore morphology probably provides the CO<sub>2</sub> access to the finest pores.

High resolution synchrotron X-ray powder diffraction data were collected at 293 K using beamline 11-BM at the Advanced Photon Source (APS), Argonne National Laboratory using an average wavelength of 0.412210 Å. Discrete detectors covering an angular range from -6° to 16° with respect to the nominal 2θ were scanned over a 34° 2θ range, with data points collected every 0.001° in 2θ at a scan speed of 0.01°/s. The instrumental optics of 11-BM incorporate two platinum-stripped mirrors and a double-crystal Si(111) monochromator, where the second crystal has an adjustable sagittal bend (Wang *et al.*, 2008b). The diffractometer is controlled via EPICS (Dalesio *et al.*, 1994). A vertical Huber 480 goniometer positions 12 perfect Si(111) analyzers and 12 Oxford-Danfysik LaCl<sub>3</sub> scintillators, with a spacing of 2° in 2θ (Lee *et al.*, 2008). Capillary samples are mounted by a robotic arm and spun at ≈90 Hz (Preissner *et al.*, 2011). Data are normalized to incident flux and collected while continually scanning the diffractometer 2θ arm. A mixture of National Institute of Standards and Technology standard reference materials, Si (SRM<sup>TM</sup> 640c) and Al<sub>2</sub>O<sub>3</sub> (SRM<sup>TM</sup> 676) is used to calibrate the instrument, where the Si lattice constant determines the wavelength for each detector. Corrections are applied for detector sensitivity, 2θ offset, and small detector wavelength differences in, before merging the data into a single set of intensities evenly spaced in 2θ.

The high-resolution pattern of ZIF-8 was fitted using the Rietveld refinement technique (Rietveld, 1969) with the software suite GSAS (Larson and von Dreele, 1992). The reference pattern was obtained with a Rietveld pattern decomposition technique. In this technique, the reported peak positions are derived from the extracted integrated

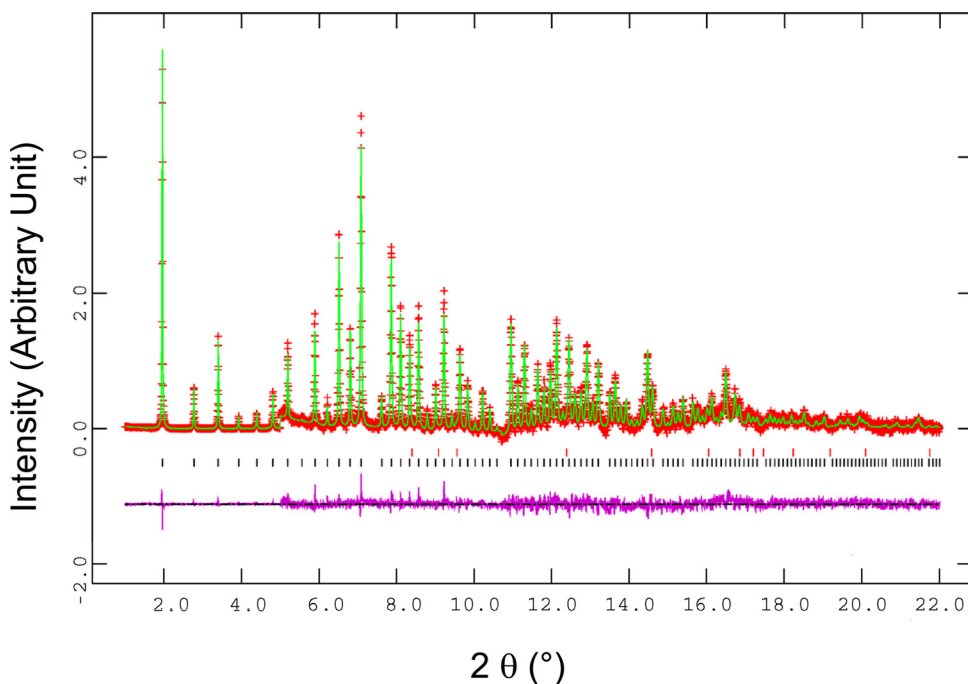


Figure 2. (Color online) Rietveld refinement results: the row of tick marks indicates the calculated peak positions. The difference pattern is plotted at same scale as the other patterns up to 5°2θ. At 5°2θ, the scale has been magnified 20 times. At 2θ values higher than 10.7°, the scale has been magnified 50 times.

TABLE I. Atomic coordinates and displacement factors for  $C_8H_{10}N_4Zn$  (cubic  $I-43m$ , with  $a = 17.01162(6)$  Å,  $V = 4932.08$  Å<sup>3</sup>, and  $Z = 12$ ). SOF represents site occupancy factor.

Atoms	$x$	$y$	$z$	$U_{iso}$	SOF
Zn1	$1/2$	1	$3/4$	0.0579 (4)	1.0
C2	0.3766 (2)	1.0082 (3)	0.6234 (2)	0.0626 (11)	1.0
C3	0.36966 (15)	0.9006 (2)	0.68626 (15)	0.0626 (11)	1.0
H4	0.3777	0.8589	0.7234	0.0813 (14)	1.0
C5	0.4045 (2)	1.0868 (3)	0.5955 (2)	0.061 (2)	1.0
H6	0.4587	1.0798	0.5743	0.080 (3)	0.5
H7	0.4058	1.1228	0.6364	0.080 (3)	0.5
H8	0.3724	1.1039	0.5525	0.080 (3)	0.5
N9	0.41156 (13)	0.9703 (2)	0.68300 (13)	0.0626 (11)	1.0

intensities and positions calculated from the lattice parameters. When peaks are not resolved at the resolution function of the diffractometer, the intensities are summed, and an intensity-weighted  $d$ -spacing is reported. Therefore, these patterns represent ideal specimen patterns. They are corrected for systematic errors both in  $d$ -spacing and intensity.

### III. RESULTS AND DISCUSSION

#### A. Crystal structure

Figure 2 gives the results of the Rietveld refinement of the ZIF-8 sample. Tick marks indicate peak positions for the main ZIF-8 phase (bottom tick marks) and a small ZnO impurity (top tick marks). The difference pattern is plotted on the same scale as the other patterns up to  $5^\circ 2\theta$ . At  $5^\circ 2\theta$ , the scale has been magnified 20 times. At  $2\theta$  values higher than  $10.7^\circ$ ,

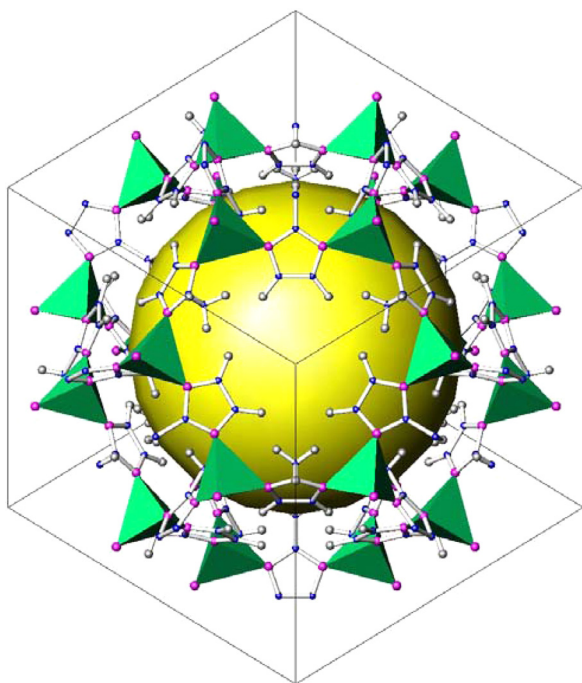


Figure 3. (Color online) Crystal structure of  $C_8H_{10}N_4Zn$ , ZIF-8, showing the large pore in a unit cell and a six-member aperture. The  $ZnN_4$  groups are shown with tetrahedral configurations (The dark spheres in the methyl groups and in the five-membered rings which are not part of the  $ZnN_4$  groups are carbon; the terminating spheres that are not filled are hydrogen). The size of the N, C, and O atoms and the pore were drawn with different scale.

TABLE II. Diffraction pattern for  $C_8H_{10}N_4Zn$  (ZIF-8) (cubic  $I-43m$ , with  $a = 17.01162(6)$  Å,  $V = 4932.08$  Å<sup>3</sup>, and  $Z = 12$ ).

$d_{cal}$ (Å)	$I_{obs}$	$h$	$k$	$l$	$d_{cal}$ (Å)	$I_{obs}$	$h$	$k$	$l$	$d_{cal}$ (Å)	$I_{obs}$	$h$	$k$	$l$
12.0290	999	1	1	0*	8.5058	126	2	0	0	6.9450	289	2	1	1
6.0145	41	2	2	0	5.3796	49	3	1	0	4.9108	132	2	2	2
4.5466	14	3	2	1	4.0097	16	4	1	1	3.8039	4	4	2	0
3.6269	42	3	3	2	3.4725	23	4	2	2	3.3362	69	4	3	1
3.1059	7	5	2	1	3.0073	45	4	4	0	2.9175	29	4	3	3
2.8353	22	4	4	2	2.7596	29	6	1	1M	2.7596	29	5	3	2M
2.6898	4	6	2	0	2.6250	11	5	4	1	2.5646	35	6	2	2
2.5082	4	6	3	1	2.4554	22	4	4	4	2.4058	13	5	4	3+
2.3150	7	7	2	1	2.2733	5	6	4	2	2.1605	13	6	5	1M
2.1605	13	7	3	2M	2.1264	6	8	0	0	2.0940	10	5	5	4M
2.0930	10	7	4	1M	2.0333	7	6	5	3	1.9776	5	8	3	1
1.9514	14	6	6	2	1.9020	11	8	4	0	1.8561	5	8	4	2
1.8344	10	9	2	1+	1.7932	7	7	5	4M	1.7932	7	8	5	1M
1.7362	7	8	4	4	1.6369	6	10	2	2	1.4377	11	10	6	2
1.4176	5	8	8	4										

the scale has been magnified 50 times. The refinement results are as follows:  $R_{wp} = 0.0711$ ,  $R_p = 0.0571$ ,  $\chi^2 = 1.295$  (28 variables, 20 999 observations),  $R(F) = 0.0509$ , and  $R(F^2) = 0.0646$ . The sample was found to contain 0.68(2) mass % of ZnO. Because of our preheat treatment of the sample prior to the synchrotron experiment, no  $H_2O$  or other solvent molecule was found in the pores.

Based on the refinement results, the space group of  $C_8H_{10}N_4Zn$  was confirmed to be cubic  $I-43m$  (Wang *et al.*, 2008a), with  $a = 17.01162(6)$  Å,  $V = 4932.08$  Å<sup>3</sup>, and  $Z = 12$ . Table I gives the atomic coordinates and displacement factors for the atoms in the structure. Figure 3 depicts the crystal structure of ZIF-8, showing the large pore and a six-member aperture. The  $ZnN_4$  groups are shown as tetrahedra. This phase was found to be highly porous (low theoretical density of  $0.92$  g/cm<sup>3</sup>). ZIF-8 contains one nanosized cavity per unit cell; the cavity is located at the center of the cell and has a diameter of about  $11.6$  Å (the largest diameter that fits into the framework without contacting the van der Waals internal surface), with  $3.5$ -Å diameter pores (Park *et al.*, 2006; Moggach *et al.*, 2009). Connected to each large nanopore are eight smaller channels.

#### B. High-resolution X-ray powder diffraction pattern

The high-resolution reference pattern is given in Table II. In this pattern, the symbols “M” and “+” refer to peaks containing contributions from two and more than two reflections, respectively. The symbol \* indicates that the particular peak has the strongest intensity of the entire pattern and has been designated a value of “999.” The intensity values reported are integrated intensities rather than peak heights. This pattern has been submitted for inclusion in the PDF.

### ACKNOWLEDGMENTS

Use of the Advanced Photon Source at Argonne National Laboratory was supported by the U. S. Department of Energy, Office of Science, Office of Basic Energy Sciences, under Contract No. DE-AC02-06CH11357. This work

utilized facilities supported in part by the National Science Foundation under Agreement No. DMR-0454672.

- Britt, D., Tranchemontagne, D., and Yaghi, O. M. (2008). "Metal-organic frameworks with high capacity and selectivity for harmful gasses," *Proc. Natl. Acad. Sci. USA* **105**, 11623.
- Chapman, K. W., Halder, G. J., and Chupas, P. J. (2009). "Pressure-induced amorphization and porosity modification in a metal-organic framework," *J. Am. Chem. Soc.* **131**, 17546–17547.
- Dalesio, L. R., Hill, J. O., Kraimer, M., Lewis, S., Murray, D., Hunt, S., Watson, W., Clausen, M., and Dalesio, J. (1994). "The experimental physics and industrial control-system architecture-past, present, and future," *Nucl. Instrum. Methods Phys. Res. A* **352**, 179–184.
- Glinka, C. J., Barker, J. G., Hammouda, B., Krueger, S., Moyer, J. J., and Orts, W. J. (1998). "The 30-m small-angle neutron scattering instruments at the National Institute of Standards and Technology," *J. Appl. Crystallogr.* **31**, 430–445.
- Larson, A. C. and Von Dreele, R. B. (1992). General Structure Analysis System (GSAS), Report LAUR 86-748, Los Alamos National Laboratory, Los Alamos, NM.
- Lee, P. L., Shu, D., Ramanathan, M., Preissner, C., Wang, J., Beno, M. A., Von Dreele, R. B., Lynn Ribaud, Kurtz, C., Antao, S. M., Jiao, X., and Toby, B. H. (2008). "A twelve-analyzer detector system for high-resolution powder diffraction," *J. Synchrotron Radiat.* **15**, 427–432.
- Lewis, D. W., Ruiz-Salvador, A., Gómez, A., Rodríguez-Albelo, L. M., Coudert, F.-X., Slater, B., Cheetham, A. K., and Mellot-Draznieks, C. (2009). "Zeolitic imidazole frameworks: Structural and energetic trends compared with their zeolite analogues," *Cryst. Eng. Comm.* **11**, 2272–2276.
- Moggach, S. A., Bennett, T. D., and Cheetham, A. K. (2009). "The effect of pressure on ZIF-8: increasing pore size with pressure and the formation of a high-pressure phase at 1.47 GPa," *Angew. Chem.* **121**, 7221–7223.
- Park, K. S., Ni, Z., Côte, A. P., Cho, J. Y., Huang, R., Uribe-Romo, F. J., Chae, H. K., O'Keeffe, M., and Yaghi, O. M. (2006). "Exceptional chemical and thermal stability of zeolite imidazolate frameworks," *Proc. Natl. Acad. Sci. USA* **103**, 10186.
- Pérez-Pellitero, J., Amrouche, H., Siperstein, F. R., Pirngruber, G., Nieto-Draghi, C., Chaplais, G., Simon-Masseron, A., Bazer-Bachi, D., Peralta, D., and Bats, N. (2010). "Adsorption of CO<sub>2</sub>, CH<sub>4</sub>, and N<sub>2</sub> on zeolitic imidazolate frameworks: Experiments and simulations," *Chem. Eur. J.* **16**, 1560–1571.
- Preissner, C., Shu, D., Toby, B. H., Lee, P., Wang, J., Kline, D., and Goetze, K. (2011). "The sample-changing robot for the 11-BM high-throughput powder diffraction beamline," *Nucl. Instrum. Methods Phys. Res. A* (in press).
- Rietveld, H. M. (1969). "A profile refinement method for nuclear and magnetic structures," *J. Appl. Crystallogr.* **2**, 65–71.
- Standard reference materials (SRM<sup>TM</sup>) are produced by National Institute of Standards SRM Office, Gaithersburg, MD 20899. For details, please contact srminfo@nist.gov.
- Wang, B., Cote, A. P., Furukawa, H., O'Keeffe, M. J., and Yaghi, O. M. (2008a). "Colossal cages in zeolite imidazolate frameworks as selective carbon dioxide reservoirs," *Nature (London)* **453**, 207.
- Wang, J., Toby, B. H., Lee, P. L., Ribaud, L., Antao, S., Kurtz, C., Ramanathan, M., Von Dreele, R. B., and Beno, M. A. (2008b). "A dedicated powder diffraction beamline at the advanced photon source: Commissioning and early operation results," *Rev. Sci. Instrum.* **79**, 085105.
- Wu, H., Zhou, W., and Yildirim, T. (2007). "Hydrogen storage in a prototypical zeolitic imidazolate framework-8," *J. Am. Chem. Soc.* **129**, 5314–5315.